






Article

The Photophysical Properties of Triisopropylsilyl-ethynylpentacene—A Molecule with an Unusually Large Singlet-Triplet Energy Gap—In Solution and Solid Phases

Fabio A. Schaberle ¹, Carlos Serpa ¹, Luis G. Arnaut ¹, Andrew D. Ward ²,
Joshua K. G. Karlsson ³, Alparslan Atahan ^{3,4} and Anthony Harriman ^{3,*}

¹ CQC, Department of Chemistry, University of Coimbra, 3004-535 Coimbra, Portugal; fschaberle@qui.uc.pt (F.A.S.); serpasoa@ci.uc.pt (C.S.); lgarnaut@ci.uc.pt (L.G.A.)

² Central Laser Facility, Research Complex at Harwell, STFC Rutherford Appleton Laboratory, Didcot OX11 0FA, UK; andy.ward@stfc.ac.uk

³ Molecular Photonics Laboratory, SNES, Newcastle University, Newcastle upon Tyne NE1 7RU, UK; joshua.karlsson@ncl.ac.uk (J.K.G.K.); alparslanatahan@duzce.edu.tr (A.A.)

⁴ Department of Polymer Engineering, Faculty of Technology, Duzce University, 81620 Duzce, Turkey

* Correspondence: anthony.harriman@ncl.ac.uk

Received: 26 April 2020; Accepted: 18 May 2020; Published: 3 June 2020



Abstract: The process of singlet-exciton fission (SEF) has attracted much attention of late. One of the most popular SEF compounds is TIPS-pentacene (TIPS-P, where TIPS = triisopropylsilylethynyl) but, despite its extensive use as both a reference and building block, its photophysical properties are not so well established. In particular, the triplet state excitation energy remains uncertain. Here, we report quantitative data and spectral characterization for excited-singlet and -triplet states in dilute solution. The triplet energy is determined to be $7940 \pm 1200 \text{ cm}^{-1}$ on the basis of sensitization studies using time-resolved photoacoustic calorimetry. The triplet quantum yield at the limit of low concentration and low laser intensity is only ca. 1%. Self-quenching occurs at high solute concentration where the fluorescence yield and lifetime decrease markedly relative to dilute solution but we were unable to detect excimer emission by steady-state spectroscopy. Short-lived fluorescence, free from excimer emission or phosphorescence, occurs for crystals of TIPS-P, most likely from amorphous domains.

Keywords: singlet exciton fission; triplet state; molecular photophysics; polyacene; photoacoustic calorimetry; excimer

1. Introduction

Around a decade or so ago, the possibility of making use of exciton multiplication, most notably in the form of singlet exciton fission (SEF), to enhance the performance of certain types of organic solar cells was formulated [1]. In fact, the concept of SEF was far from new at that time, but was generally considered a scientific curiosity, of which the field of molecular photophysics is richly endowed [2]. The prospect of advanced applications, in addition to the enormous challenge to provide a theoretical framework by which to explain and exploit SEF, fueled a rapid acceleration in interest in the field and resulted in considerable diversification. Originally, SEF was thought to be restricted to higher-order polyacenes [3], such as tetracene [4], pentacene [5] and hexacene [6], but many other classes of organic chromophores were identified as promising SEF candidates. Michl, for example, recognized the SEF capabilities of indigoids [7] and benzofurans [8], but a wealth of other promising compounds has been uncovered. Throughout this growth period, two research themes have been at the forefront of the field,

regardless of the molecular architectures being proposed, and these refer to: (i) the level of electronic coupling between pairs of adjacent chromophores [9,10] and (ii) the underlying thermodynamics, or energy balance, governing the SEF process [11,12]. In crude terms, it is generally considered that the excitation energy of the relaxed singlet exciton must exceed twice the excitation energy of the resultant triplet exciton for SEF to be efficacious [13]. This latter requirement raises an important issue in as much as there are severe experimental difficulties associated with accurate determination of triplet energies in the region of ca. 1 eV and less.

Here, we are concerned with a prototypic SEF compound, namely TIPS-pentacene (TIPS = triisopropylsilylethynyl) [14], which has figured prominently in recent SEF history. The TIPS group is used primarily to improve solubility but it also affects the electronic properties of the chromophore [15]. It has been demonstrated repeatedly that pentacene derivatives are excellent materials for SEF in devices [16], thin films [17] and highly concentrated solutions [18] and also as components of covalently-linked molecular bichromophores [19–22]. Despite this inherent popularity, the photophysical properties of isolated TIPS-pentacene (TIPS-P) have not been so well documented and, in particular, the triplet excitation energy remains a matter of some uncertainty. The latter is of crucial significance in establishing the SEF energy balance, especially since it has to be recognized that SEF can lead to formation of isolated triplets as well as triplet biexcitons [23–25]. It is also essential to determine the inherent intersystem-crossing properties in the absence of SEF so that the true benefit of the SEF event can be established.

It is universally accepted that SEF in TIPS-P is mildly exergonic, that is to say that the bulk of the singlet excitation energy can be accommodated in the triplet biexciton [26], at least in cases where the yield of the triplet biexciton approaches 100%. Smith and Michl [3] reviewed in considerable detail the optical properties of the parent pentacene (Pn), and determined a preferred triplet excitation energy of 0.86 eV for solid pentacene. This value is derived from the activation energy of heterofission with Pn as a guest in a solid matrix and also from direct measurement on a thin film. Low-temperature phosphorescence from Pn in a frozen cyclohexane matrix gives a slightly higher triplet energy of 0.95 eV [27]. This latter value, which in all likelihood refers to an isolated Pn molecule, might be considered as an upper limit for the triplet energy of TIPS-P. Recent calculations of the vertical triplet energy of Pn indicate a value of 0.88 eV [28], in close agreement with the experimental results. In addition, there are two reports of low-temperature phosphorescence from TIPS-P in frozen media. One such account compares phosphorescence from TIPS-P with that from a covalently-linked bichromophore [19] and reports the phosphorescence maximum at 1580 nm (i.e., 0.78 eV). In this experiment, TIPS-P was studied as a dilute solution in 2-methyltetrahydrofuran at 77K, where the solvent forms a rigid glass. The second report [29] refers to phosphorescence from TIPS-P in deoxygenated toluene at 77K. The emission peak also lies at 1580 nm, while the phosphorescence lifetime was reported as being 12.9 μ s. Notably, the singlet excitation energy of Pn and TIPS-P in 2-methyltetrahydrofuran, respectively, is 2.13 eV and 1.92 eV. A bandgap of 1.83 eV has been reported for films prepared from TIPS-P [14].

In this contribution we report quantitative photophysical properties for TIPS-P in dilute solution. The main purpose of the work is to provide a complete set of values relevant to liquid solution and to obtain an independent estimate for the triplet excitation energy under ambient conditions. Our concern about the triplet energy derived from low-temperature phosphorescence spectra relates to the very low triplet yield formed under these conditions. As will be shown below, in de-aerated toluene, inherent intersystem crossing to the triplet manifold is barely detectable at room temperature and is hardly likely to increase at 77 K. Considerable interest from both theoretical and experimental approaches has been directed towards improved clarification of the various triplet excitons that might be encountered throughout the entire SEF process [23–25]. These include isolated triplets, spin coherent pairs, quintets and so on and an increasing variety of spectroscopic techniques, including vibrational [30] and magnetic [31] probes, are being applied to monitor the triplet state. Additional

studies are addressing aspects of competition between SEF and light-induced electron transfer [20]. An independent assessment of the spectroscopic properties appears to be in good order.

2. Materials and Methods

Samples of TIPS-pentacene (TIPS-P) were synthesized in-house using a standard protocol [32] (Figure 1). Additional samples were purchased from Sigma-Aldrich (Gillingham, UK) and used as received. No obvious differences were observed. Samples of 5,10,15,20-tetrakis(2,6-difluoro-3-*N*-methylsulfamoyl-phenyl)bacteriochlorin, referred to throughout as redaporfin, were provided by Luzitin SA (Coimbra, Portugal) and were used without further purification. Toluene (Aldrich, 99.9% and Fisher, Loughborough, UK, 99.97%) was used as the solvent. Oxygen was removed either by purging with O₂-free nitrogen or by several freeze-pump-thaw cycles on a high vacuum line. Iodoethane was purchased from Sigma-Aldrich and passed down a short alumina column before use. It was stored at 4 °C in the dark. All solutions were prepared fresh.

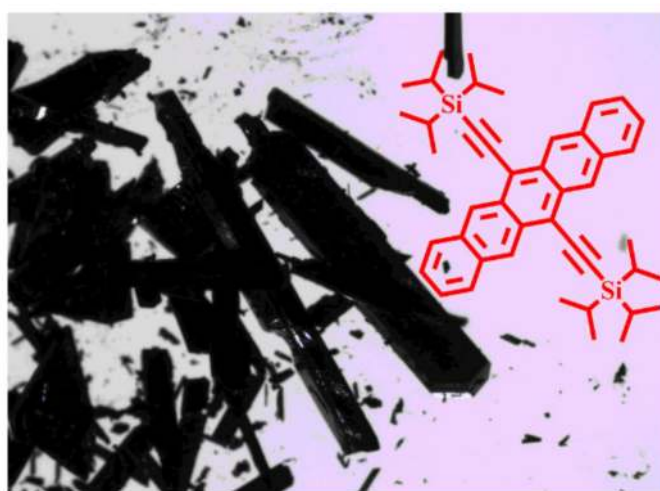


Figure 1. Chemical formula for TIPS-P superimposed over a photograph of crystals of the same material.

Absorption spectra were measured with either a UV-2100 spectrophotometer (Shimadzu, Kyoto, Japan) or with a U3310 spectrophotometer (Hitachi, Tokyo, Japan). Steady-state fluorescence measurements were recorded using a Fluorolog Tau-3 system (Horiba, Kyoto, Japan) equipped with a water-cooled R2658P photomultiplier detector. Time-resolved fluorescence decay measurements were recorded with a time-correlated, single photon counting system, where excitation was with a 635 nm short-pulse laser diode. Time-resolved absorption measurements were obtained with an LKS-70 system (Applied Photophysics, Leatherhead, UK) using a 4-ns pulsed Brilliant B Nd:YAG laser (Quantel, Lannion, France) with the 1067 nm output being frequency doubled to give 534 nm. The repetition rate of the laser was 10 Hz with the power varying from 1–100 mJ per pulse. Fluorescence quantum yields were measured using meso-tetraphenyl porphyrin as a standard ($\Phi_F = 0.11$ in toluene) [33]. All photophysical measurements were repeated at least three times.

Photoacoustic calorimetry (PAC) experiments employed a homemade, front-face irradiation cell [34]. As necessary, samples were saturated with nitrogen for 20 min before starting the measurement. The sample, reference and solvent solutions were flowed separately using a syringe pump (Kloehn, Littleton, CO, USA) through the 0.11 mm thick photoacoustic cell. They were irradiated at 695 nm (redaporfin + TIPS-P) or 643 nm (TIPS-P) with an OPO (PG122/SH, Ekspla, Vilnius, Lithuania) pumped by the third harmonic of a nanosecond Q-switched Nd:YAG laser (Ekspla NL301G), working at a frequency of 10 Hz. The maximum energy per pulse was less than 1.0 mJ in all experiments. The photoacoustic waves were detected by a 2.25 MHz Panametrics transducer (model 5676, Olympus, Tokyo, Japan), amplified by a preamplifier, recorded by a digital oscilloscope (DPO7254C, Tektronix, Beaverton, OR, USA) and transferred to a PC for data analysis and storage. Analysis of the photoacoustic

waves were performed with CPAC software [35]. In each PAC experiment, 200 waves were averaged for each sample, reference and solvent in the same experimental conditions, and four different laser intensities were used. Neutral density filters were employed to obtain the different laser intensities. All measurements were made in toluene using azulene as photoacoustic calorimetry reference [36].

For the NIR emission studies, laser light (532 nm) from a Verdi V8 laser (Coherent, Santa Clara, CA, USA) was focused onto the sample through an x63 water immersion objective lens (NA 1.2, Leica, Wetzlar, Germany). A variable neutral density filter was used to attenuate the laser, such that 2 mW laser power was present at the beam focus. The emission signals were collected using the same objective lens, i.e., backscattered light, and a long pass dichroic mirror (DMLP1000, Thorlabs, Ely, UK) was used to reject all light below 985 nm. The signal was detected using an NIR spectrograph (Isoplan SCT-320, Acton Research Company, Acton, MA, USA) combined with an InGaAs array detector (NIRvana 640, Princeton Instruments, Trenton, NJ, USA). Acquisition times were typically 1 s. A 300 groove/mm grating blazed at 1.2 microns was used for all spectral measurements. The spectrograph was calibrated using the gas emission lines of a mercury-argon PenRay discharge lamp (Thorlabs, Ely, UK). The overall configuration of the spectrometer was similar to that described earlier [37].

3. Results

3.1. Photophysics in Dilute Solution

The absorption spectrum recorded for TIPS-P at micromolar concentration in toluene is shown as Figure 2. The 0,0 absorption transition (λ_{ABS}) can be located at 643 nm, where the molar absorption coefficient (ϵ_{MAX}) is $23,250 \text{ M}^{-1} \text{ cm}^{-1}$. The Beer-Lambert law is followed over a modest concentration range (Figure 2). Fluorescence is observed following excitation into the lowest-energy absorption transition and has a maximum (λ_{FLU}) at 652 nm. This corresponds to a Stokes shift of only 215 cm^{-1} . There is excellent agreement between absorption and excitation spectra over the wavelength range of interest (Figure 2).

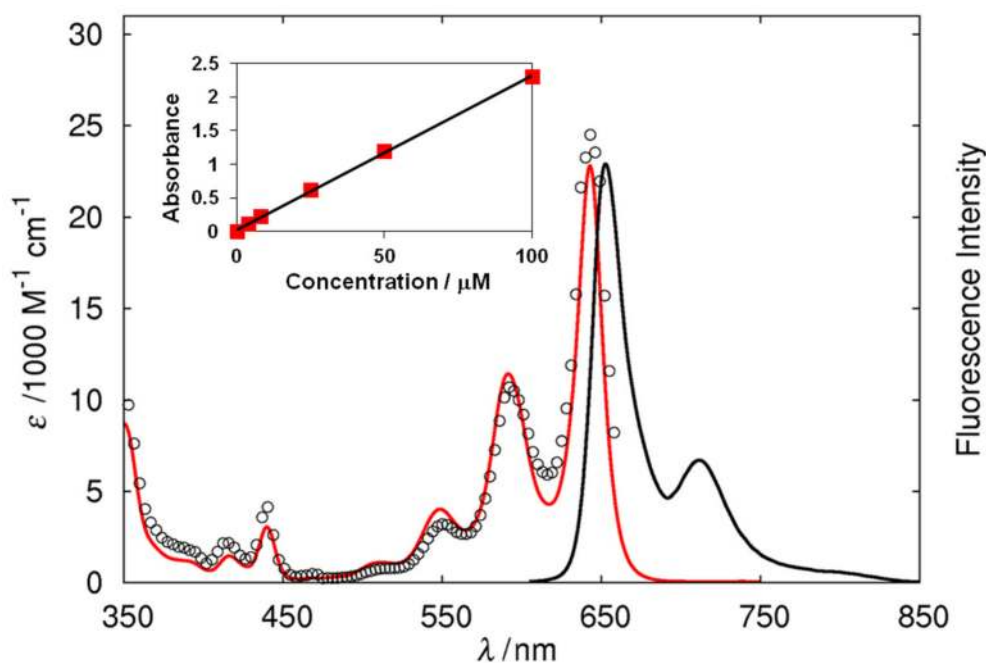


Figure 2. Absorption (red curve), fluorescence (black curve) and excitation (open circles) spectra recorded for TIPS-P in toluene. The inset shows a Beer-Lambert plot over the concentration range of interest; absorbance values greater than unity were measured in 2 mm path lengths cells and rescaled.

The fluorescence quantum yield (Φ_F) determined in air-equilibrated toluene was found to be 0.75 ± 0.03 while the excited-singlet state lifetime (τ_S) was measured by time-correlated, single-photon counting to be 14 ± 1 ns. In degassed toluene, Φ_F increases to 0.92 ± 0.04 while τ_S is prolonged to 22 ± 2 ns (Figure 3a). The natural lifetime calculated from the Strickler-Berg expression [38] is 24 ns. Literature reports for τ_S in toluene solution include values of 17 ns [20] and 13 ns [19].

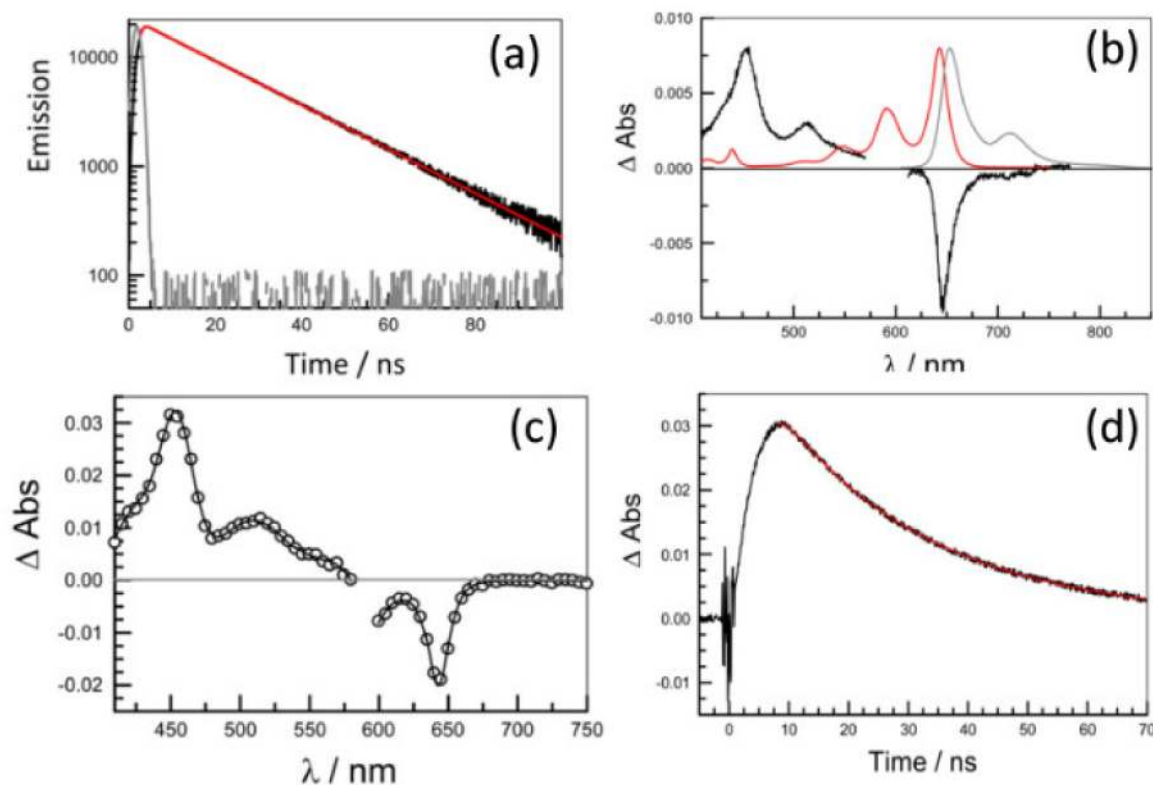


Figure 3. (a) Fluorescence decay curve recorded by time-correlated, single photon counting methods following excitation at 635 nm. The experimental data appear as a solid black line with the non-linear least-squares best fit superimposed as a red line. The instrument response function is shown in grey. (b) Example of a transient differential absorption spectrum recorded 5 ps after excitation of TIPS-P in toluene at 590 nm (FWHM = 0.2 ps) (black curve), together with the ground-state absorption spectrum (red curve) and the S_1 - S_0 fluorescence spectrum (grey curve). (c) Example of a S_1 - S_N transient differential absorption spectrum recorded for TIPS-P in de-aerated toluene following excitation with a 4-ns laser pulse at 585 nm. The spectrum was recorded after a delay time of 10 ns. (d) Example of a kinetic decay curve recorded at 455 nm following 4-ns laser excitation of TIPS-P in de-aerated toluene at room temperature.

Excitation of TIPS-P in de-aerated toluene with a short laser pulse (FWHM = 0.2 ps) at 590 nm populates the corresponding excited-singlet state. Differential transient absorption spectra recorded soon after excitation show pronounced bleaching around 650 nm together with absorption in the region of 455 nm (Figure 3b). The bleaching signal corresponds to transient loss of the ground-state chromophore together with a substantial crop of stimulated emission. The absorption band centred at 455 nm can be assigned to the S_1 - S_N transition. Decay of the S_1 state follows first-order kinetics with a lifetime of ca. 15 ns but decay is incomplete over the available time window of 6 ns. To confirm that deactivation of the S_1 state restores the pre-pulse baseline, excitation was made with a 4-ns laser pulse delivered at 585 nm (Figure 3c). Under these conditions, the excited state decays via first-order kinetics with an average lifetime of 26 ± 4 ns in de-aerated toluene (Figure 3d).

The S_1 state shows slight absorption in the region of strong ground-state bleaching such that the differential molar absorption coefficient ($\Delta\epsilon_{455}$) at 455 nm should not be obtained simply by

comparison to that of the ground-state at the maximum of 643 nm. In this respect, the spectrum obtained after excitation with the 4-ns pulse is more useful because of the absence of stimulated emission and the slightly extended bleaching region. Matching bleaching of the ground state with the corresponding absorption spectrum leads to a value for $\Delta\epsilon_{455}$ of $37,200 \text{ M}^{-1} \text{ cm}^{-1}$, which is well within experimental error of the value obtained earlier by pulse radiolysis ($\Delta\epsilon_{455} = 38,250 \text{ M}^{-1} \text{ cm}^{-1}$) [22]. The transient differential absorption spectrum recorded here is in good agreement with that reported by Wasielewski et al. [20] in both fluid solution and thin films, where the derived molar absorption coefficient at the band maximum of 481 nm (in a thin film!) was $33,300 \text{ M}^{-1} \text{ cm}^{-1}$. Our derived $\Delta\epsilon_{455}$ is significantly smaller than that obtained by Guldi et al. [19], where the peak absorbance at 447 nm was assigned $\Delta\epsilon_{447}$ of $83,000 \text{ M}^{-1} \text{ cm}^{-1}$.

Iodoethane quenches fluorescence from TIPS-P and promotes population of the excited-triplet state by way of the external heavy atom effect [20,39]. A non-linear Stern-Volmer plot is recovered for the addition of iodoethane to TIPS-P in 2-methyltetrahydrofuran solution. However, the data are well explained in terms of static quenching. Excitation of TIPS-P in de-oxygenated toluene containing 20% (*v/v*) iodoethane populates the triplet-excited state as evidenced by the appearance of the characteristic T_1 - T_3 absorption spectrum [3]. In fact, the derived differential absorption spectrum (Figure 4) closely resembles that reported for Pn by Porter et al. [40] in the 1950s as well as the spectrum recorded for TIPS-P by pulse radiolysis in toluene [22].

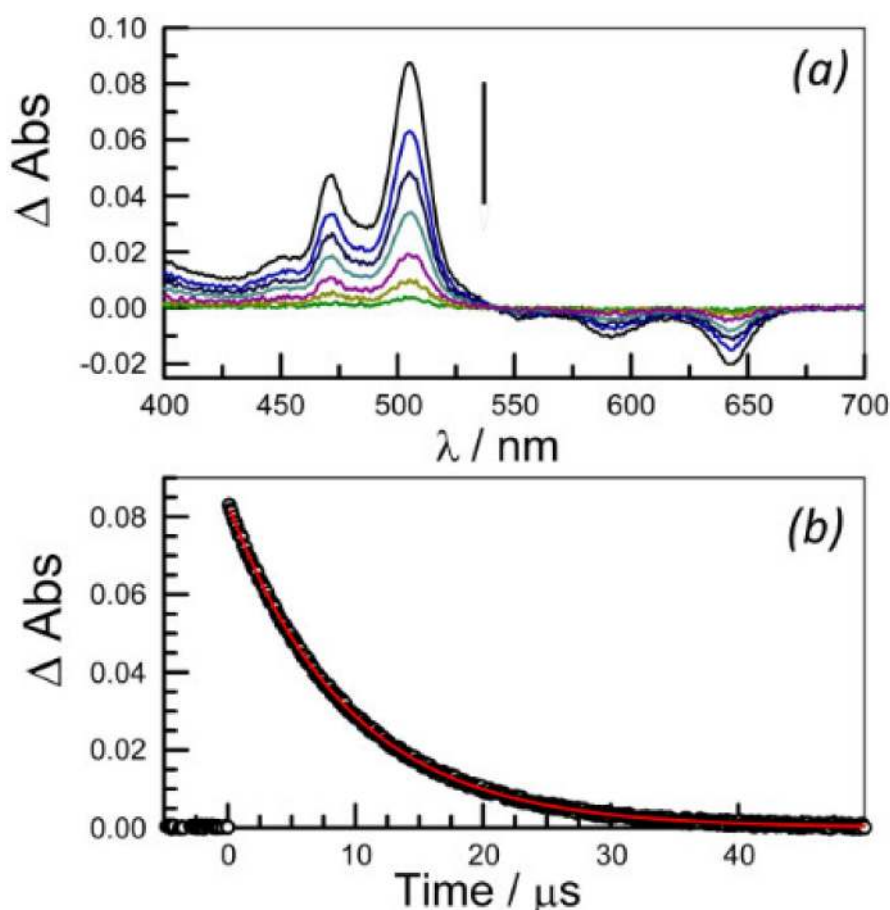


Figure 4. (a) Transient differential absorption spectra recorded at various times after laser excitation with a 4-ns pulse at 590 nm of TIPS-P in de-aerated toluene containing 20% *v/v* iodoethane. The arrow indicates increasing time delay. (b) Example of a decay kinetic trace recorded at 505 nm for the experiment described in (a). The experimental data are shown as open circles with the non-linear, least-squares best fit shown as a super-imposed red line.

The corresponding T_1 - T_2 transition is dipole forbidden and has been the subject of considerable theoretical discussion. This latter transition is expected to appear in the region around 900 nm [12] but has proven difficult to detect. Under our conditions, the triplet lifetime (τ_T) is $9 \pm 2 \mu\text{s}$ but is sensitive to the concentration of residual oxygen. This lifetime decreases as more iodoethane is added, allowing extrapolation of τ_T in the absence of spin-orbit accelerant as being ca. 40 μs . This can be compared to literature values of 24 μs [19] and 6.5 μs [18]. The latter value was obtained for a concentrated solution of TIPS-P in toluene but it is known that the triplet state is quenched by ground-state TIPS-P.

The triplet differential absorption spectrum exhibits positive signals in the region of 500 nm and bleaching of the ground-state absorption bands at longer wavelength. On the basis that the triplet state does not absorb around 650 nm, we can determine the differential molar absorption coefficient ($\Delta\epsilon_{505}$) for the triplet at 505 nm. The derived value is $81,500 \text{ M}^{-1} \text{ cm}^{-1}$ which is somewhat smaller than that determined by actinometric pulse radiolysis [22]. Literature values for $\Delta\epsilon_{505}$ are usually based on comparison with ground-state bleaching in the red region and include $64,000 \text{ M}^{-1} \text{ cm}^{-1}$ [20] and $160,000 \text{ M}^{-1} \text{ cm}^{-1}$ [19]. In part, these discrepancies arise from variations in the molar absorption coefficient for the ground state; our measured ground-state value at 643 nm ($\epsilon_{\text{GS}} = 23,250 \text{ M}^{-1} \text{ cm}^{-1}$) is higher than that reported by Anthony et al. ($\epsilon_{\text{GS}} = 20,000 \text{ M}^{-1} \text{ cm}^{-1}$) [14], which is used as standard by many research groups. A value for ϵ_{GS} of $21,000 \text{ M}^{-1} \text{ cm}^{-1}$ has been recorded for concentrated solutions of TIPS-P in toluene [18] while the anomalously high value of $33,000 \text{ M}^{-1} \text{ cm}^{-1}$ was preferred by Guldi et al. [19]. Interestingly, although the absolute values for ϵ_{455} and ϵ_{505} differ significantly, the ratio remains close to 2 in each case. It is this ratio that is often used to establish yields for SEF. An additional problem encountered with SEF concerns distinguishing between isolated triplets and triplet biexcitons [23–25].

Having established what we believe are reliable descriptions of the excited-singlet and -triplet state transient absorption spectra, attention now turns to determination of the inherent triplet yield and the triplet excitation energy. In the absence of a spin orbit accelerant, excitation of TIPS-P in de-aerated toluene does not give a measurable yield of the triplet state. This same problem was encountered by Wasielewski et al. [20]. However, the triplet can be populated indirectly by way of triplet-triplet electronic energy transfer [22]. For this purpose, redaporfin [41] was used as the triplet donor.

Shown in Figure 5 are examples of transient absorption spectra obtained following laser excitation of a mixture of redaporfin (11 μM) and TIPS-P (100 μM) in de-aerated toluene at an excitation wavelength of 355 nm. Under these conditions, redaporfin absorbs ca. 65% of the incident photon flux but it has already been established that direct excitation of TIPS-P does not lead to triplet formation in any measurable yield. The initial transient absorption profile corresponds closely to that of the redaporfin triplet-excited state [41]. As the donor triplet decays, there is concomitant appearance of the spectral features characteristic of the triplet-excited state of TIPS-P. These observations are consistent with triplet-triplet electronic energy transfer from redaporfin to TIPS-P.

The triplet lifetime of redaporfin, monitored at 530 nm by way of ground-state recovery [42], where TIPS-P makes little contribution to the overall signal, decreases from 55 μs in the absence of TIPS-P to 18 μs in the presence of the acceptor (at a concentration of 63 μM (Figure 5)). Monitoring at 500 nm, where TIPS-P triplet is the dominant absorber, shows a rise-time of 17 μs , analogous to the decay of the redaporfin triplet observed at 530 nm (Figure 6), followed by a 46 μs decay. It is notable that, although TIPS-P makes an important contribution to the total absorbance at 355 nm, appearance of the triplet state is entirely the result of electronic energy transfer. This observation confirms the studies described above.

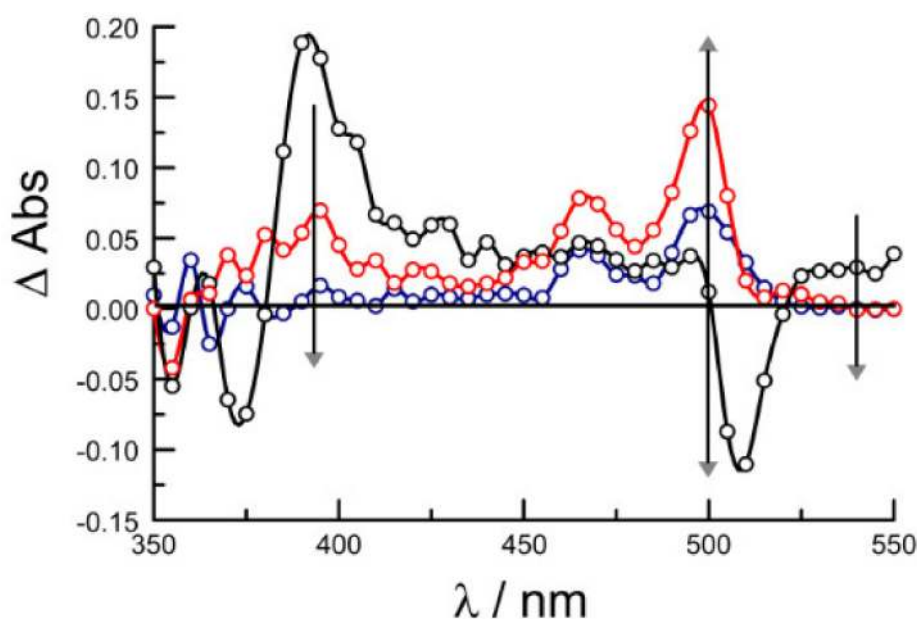


Figure 5. Transient absorption spectra for redaporfin in the presence of TIPS-P in de-aerated toluene with laser excitation at 355 nm. Individual spectra were recorded at delay times of 2.4 μs (black), 15.2 μs (red) and 50.4 μs (blue). The downwards arrows indicate wavelengths at which the redaporfin triplet can be monitored. The arrow at 500 nm indicates growth and subsequent decay of TIPS-P triplet.

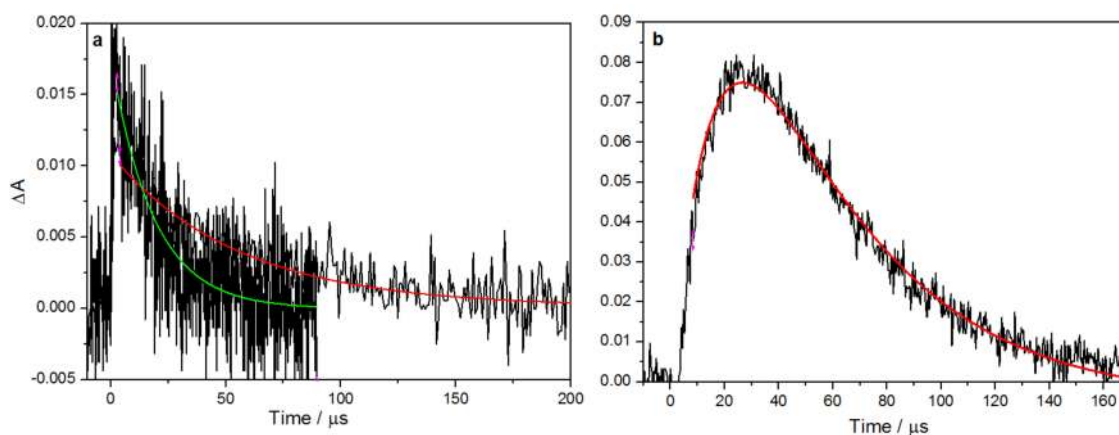
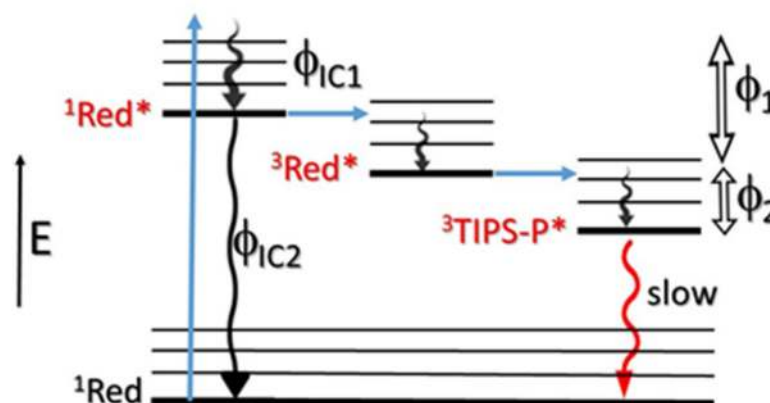


Figure 6. Transient differential absorption kinetic decays recorded for redaporfin in de-aerated toluene at room temperature. (a) Decay recorded at 530 nm in the absence of TIPS-P (red curve), where the lifetime is 55 μs , and in the presence of TIPS-P at a concentration of 63 μM (green curve). In the latter case the triplet lifetime of redaporfin is reduced to 18 μs . (b) Kinetic trace recorded at 500 nm, where the triplet state of TIPS-P dominates the spectral records. With [TIPS-P] = 63 μM , the measured rise-time constant is 17 μs and the subsequent decay time constant is 46 μs .

The above observation raises the question as to how it is possible to observe low-temperature phosphorescence from TIPS-P [19,28] in the absence of a spin-orbit coupling activator. Our own attempts to detect phosphorescence failed to produce any convincing spectral features in the region of 1600 nm and attention therefore turned to a different experimental method that might allow meaningful determination of the triplet energy. It seems instructive to mention here that we did succeed at detecting room-temperature phosphorescence from a covalently-linked TIPS-P bichromophore [22] and this will be described later in a separate publication.

An alternative method for obtaining triplet energies is provided by photoacoustic calorimetry, which gives information on the quantity of heat released by way of radiationless deactivation of an

excited state [43–47]. For this experiment, redaporfin was used as triplet energy donor. Here, selective excitation of the donor generates the donor singlet-excited state which decays within the temporal resolution of the instrument to yield the corresponding triplet-excited state by way of “very fast” intersystem crossing (Scheme 1). In the presence of high concentrations of TIPS-P, electronic energy transfer from triplet redaporfin leads to evolution of triplet TIPS-P. Given that the triplet energy of redaporfin is 9090 cm^{-1} [41], triplet-triplet energy transfer is an exergonic process and the associated enthalpy change will contribute to the total photoacoustic signal. At the highest TIPS-P concentrations, triplet quenching is quantitative so that the yield of the TIPS-P triplet state equals the initial concentration of triplet redaporfin. The time resolution set by the 2.25 MHz transducer covers the range 20 ns to 1 μs . The subsequent decay of TIPS-P triplet occurs over a few tens of microseconds and therefore is too “slow” to be detected (Scheme 1).



Scheme 1. Illustration of the various energy loss steps associated with excitation and decay processes following excitation of redaporfin in the presence of TIPS-P. NB ϕ_{IC1} has a value of unity while ϕ_{IC2} for redaporfin is 0.212. The quantum yield for intersystem crossing in the redaporfin molecule is 0.65. Recall radiationless decay from the TIPS-P triplet state, shown as a red arrow, is too slow to be monitored by our PAC set-up.

The “very fast” heat decay associated with generation of the triplet state of redaporfin is separated from its “fast” quenching by TIPS-P, which is separated from the “slow” decay of the TIPS-P triplet. The “very fast” processes contribute to the first fraction of heat detected (ϕ_1), the “fast” processes contribute to the second fraction (ϕ_2) and the “slow” processes are not detected by our set-up. Hence, in these particular experiments, two consecutive decays can be isolated, corresponding to: (i) formation of redaporfin triplet state, and (ii) subsequent triplet-triplet energy transfer from redaporfin to TIPS-P. We are especially concerned with the electronic energy transfer step described by Equation (1) since this value provides access to the triplet excitation energy of TIPS-P. Here, Φ_T ($= 0.65$) is the quantum yield for formation of the triplet-excited state of redaporfin [41,42]. In order to ensure that only redaporfin is excited, an excitation wavelength of 695 nm was used. Finally, the TIPS-P concentration was selected to be sufficiently high so as to ensure that more than 95% of the initial redaporfin triplet population was quenched by way of electronic energy transfer.

$$\phi_2 E_{hv} = \Phi_T [E_T(\text{Red}) - E_T(\text{TIPS-P})] \quad (1)$$

Shown in Figure 7a are solvent corrected and normalized photoacoustic waves obtained for azulene as photoacoustic reference [48] and for the mixture of redaporfin and TIPS-P. The experimental data were fitted according to two consecutive decays with the associated four parameters (ϕ_1 , τ_1 , ϕ_2 , τ_2) allowed to float freely. The best fit yielded an initial decay with $\tau_1 < 10\text{ ns}$ (i.e., faster than the time resolution of the 2.25 MHz detector) and a slower component with $\tau_2 \approx 100\text{ ns}$. This longer lifetime is consistent with the TIPS-P concentration employed and with a bimolecular quenching rate constant

of ca. $10^9 \text{ M}^{-1} \text{ s}^{-1}$. The open square and circle symbols relevant to Figure 7a represent the calculated waves obtained by fitting of the experimental photoacoustic wave. A simulation of the photoacoustic wave is presented as Figure 7b. The average values derived for ϕ_1 , ϕ_2 and τ_2 , as well as the parameters used to calculate the triplet energy (E_T) of TIPS-P, are collected in Table 1. The final value for E_T of TIPS-P calculated with Equation (1) is $7940 \pm 1200 \text{ cm}^{-1}$, while the lifetime of the quenched triplet of redaporfin is ca. 110 ns for both TIPS-P concentrations employed here.

$$\phi_1 E_{hv} = E_{S1} - E_{S1} + \phi_{IC2} E_{S1} + \Phi_T [E_{S1} - E_T] + \Phi_F \Delta E_r \quad (2)$$

$$E_T \Phi_T = E_{hv} (1 - \phi_1) - \Phi_F E_{vmax} \quad (3)$$

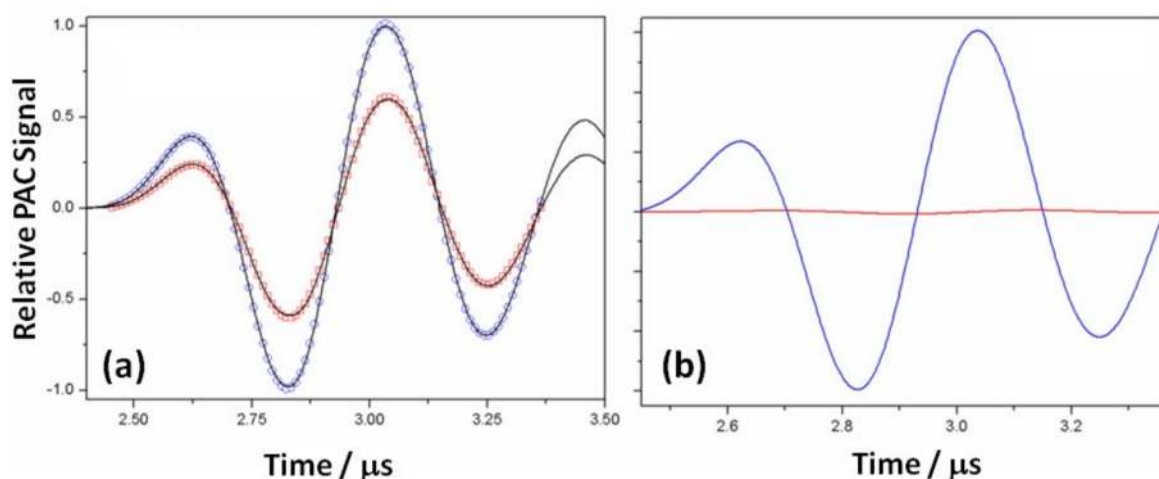


Figure 7. (a) Solvent corrected, normalized photoacoustic waves and their subsequent fitting for azulene (reference wave given in blue) and for redaporfin in the presence of TIPS-P at a concentration of 1.0 mM in de-aerated toluene (sample curve given in red). The excitation wavelength was 695 nm. (b) Simulated photoacoustic waves depicting the curves generated by the energy fractions of $\phi_1 = 0.576$ ($\phi_1 < 10 \text{ ns}$; blue curve) and $\phi_2 = 0.051$ (mean $\tau_2 = 110 \text{ ns}$; red curve).

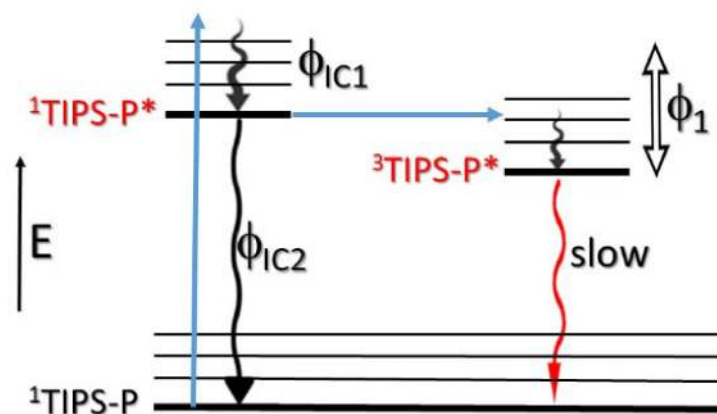
Table 1. Summary of the main findings relating to the photoacoustic calorimetry investigation of the redaporfin sensitized triplet formation for TIPS-P in de-aerated toluene following laser excitation at 695 nm ($E_{hv} = 14370 \text{ cm}^{-1}$).

[TIPS-P]/mM	ϕ_2	E_T/cm^{-1} ¹
1.00	0.0527 ± 0.0079	7940 ± 1190
2.50	0.0519 ± 0.0072	7940 ± 1080

¹ Refers to the lowest-energy, triplet excited state of TIPS-P.

The derived E_T for TIPS-P can be used [35,36,46] to estimate the quantum yield for nonradiative deactivation of the excited-singlet state. It will be recalled that our estimate for the fluorescence quantum yield in degassed toluene and air-equilibrated solution ($\Phi_F = 0.92$ and 0.75 , respectively) implies that radiationless decay will be small for TIPS-P at low concentration. Scheme 2 depicts the processes relevant to such conditions ($[\text{TIPS-P}] < 10 \mu\text{M}$) when TIPS-P is excited directly at 643 nm (i.e., $15,560 \text{ cm}^{-1}$). In air-equilibrated solution, the very fast formation of TIPS-P excited-singlet state leads to state depopulation by three distinct processes: fluorescence, intersystem crossing to the triplet manifold and internal conversion to reform the ground state. The nonradiative deactivation processes are detected as a prompt photoacoustic signal and Equations (2) and (3) can be used to describe the fraction of prompt heat (ϕ_1) released [46]. The ground state recovered by fluorescence also relaxes in this time window and contributes to the photoacoustic signal ($\Phi_F \times \Delta E_r$). On the assumption that ϕ_{IC1}

is unity and on extrapolation to zero laser power, the final conclusion is that Φ_T under these conditions is less than a few percent (Table 2). This is fully consistent with our failure to detect significant triplet population on direct excitation of TIPS-P.



Scheme 2. Illustration of the expected photophysical steps following direct excitation of TIPS-P in dilute solution.

Table 2. Results of the photoacoustic calorimetry studies made for direct excitation of TIPS-P in toluene with a laser pulse delivered at 643 nm ($E_{hv} = 15,550 \text{ cm}^{-1}$).

[TIPS-P]/ μM	$E_{\text{max}} \times \Phi_F/\text{cm}^{-1}$ ¹	φ_1	Φ_T ²
5.2	11,505	0.2556 ± 0.0119	0.0087 ± 0.0004
8.4	11,505	0.2636 ± 0.0060	-0.0068 ± 0.0001

¹ Corresponds to the energy at the maximum fluorescence intensity of TIPS-P ($E_{\text{max}} = 15,355 \text{ cm}^{-1}$) multiplied by the fluorescence quantum yield. ² Refers to the quantum yield for inherent population of the triplet excited state of TIPS-P.

3.2. Luminescence from Crystalline Samples

Because SEF is known to be efficacious for thin films [16,17,49,50], crystals [51–53] and aqueous suspensions of nanoparticles [54], it was decided to search for room temperature phosphorescence from crystals of TIPS-P. Large crystals were grown from the minimum volume of chloroform (Figure 1). The absorption spectrum recorded for these crystals remains similar to that observed for dilute solution except for the appearance of a band in the far-red region (Figure 8). This latter band, which is centred at 730 nm and is relatively broad, is clearly a consequence of moving to the solid state. No such absorption band could be seen at high concentration in solution (see below) but a low-energy absorption transition, centred at 1.75 eV (i.e., 710 nm), has been reported for thin films of TIPS-P prepared by drop-casting [55,56]. The position and width of the low-energy absorption band will depend on the structure and morphology of the sample, with less pronounced red shifts expected for amorphous domains compared to polycrystalline films. Our interpretation of the optical spectra recorded for our crystals allows for amorphous domains, perhaps at the surface, where the chromophore retains optical properties somewhat comparable to solution. The crystalline regions are responsible for the red-shifted absorption maximum but also absorb at higher energies. Both the thin film and the crystal show signs of light scattering in the near-UV region.

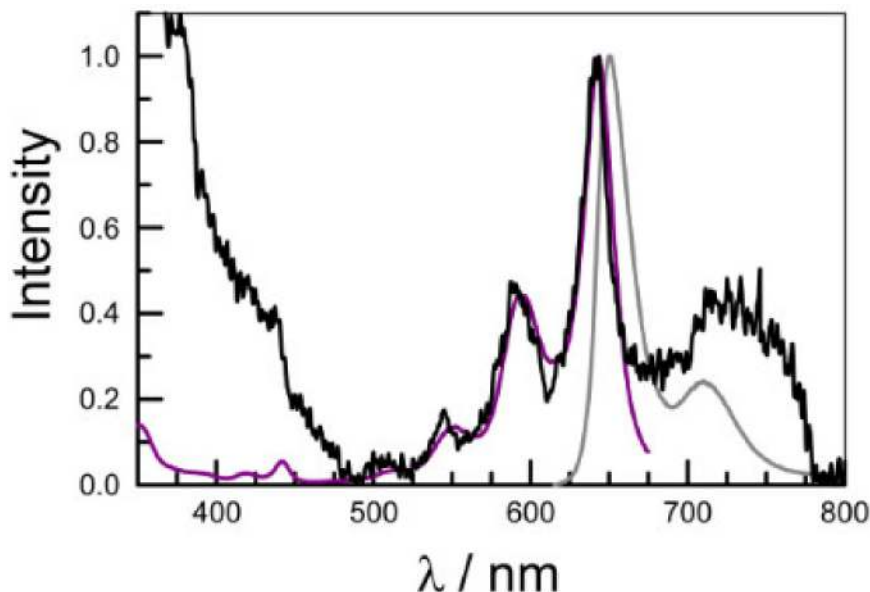


Figure 8. Absorption spectrum (black curve) recorded for a single crystal of TIPS-P; note the maximum absorbance at wavelengths longer than 400 nm did not exceed 0.25. Also given are the fluorescence spectrum (grey curve) for excitation at 620 nm and the excitation spectrum (indigo curve) for emission at 720 nm. The spectra are normalized at the respective maxima in the red region.

Weak fluorescence could be detected from our crystals of TIPS-P following excitation at 635 nm (Figure 8). The spectral profile closely resembles that recorded for dilute solutions with the emission maximum appearing at 650 nm. The excitation spectrum is in good agreement with the absorption spectrum recorded for the crystal but is not contaminated by scattering effects. Following excitation at 635 nm, time-resolved emission decay curves fit reasonably well as single-exponential processes with a lifetime of 138 ± 25 ps.

This lifetime is heavily quenched compared to that recorded for dilute solutions. As mentioned above, this emission is assigned to TIPS-P molecules resident in amorphous domains. The fluorescence quantum yield estimated using an integrating sphere and excitation with a laser diode emitting at 632 nm is reduced to <3%. Fluorescence from polycrystalline films of TIPS-P [55,56] has been reported, but again the quantum yield and lifetime were found to be greatly reduced relative to solution. An S_1 lifetime of 250 ps has been reported following excitation of the film at ca. 700 nm, and assigned to exciton recombination, but transient absorption spectral studies indicated the co-existence of much faster decay processes [56]. These latter light-induced deactivation steps relate to TIPS-P molecules associated with highly crystalline domains. For our samples, excitation at 700 nm selectively addresses the crystalline regions. Under such conditions, fluorescence was difficult to resolve from the baseline and no quantitative measurements could be made.

Examination of a single crystal of TIPS-P under an optical microscope shows that ablation occurs on illumination at 532 nm, a wavelength that probes both amorphous and crystalline domains, even at moderate (i.e., 30 mW) laser power. The edges of the crystal corrode under excitation and the fluorescence fades over a few tens of seconds. With a much reduced (i.e., 2 mW) laser power, ablation is subdued. Under such conditions, it appears that the tail of the fluorescence extends as far as 1500 nm (Figure 8), despite the strong quenching. We attribute fluorescence to TIPS-P molecules resident in amorphous regions of the crystal, perhaps associated with the surface. Comparable signals were observed with a range of different crystals. It was not possible to gate the spectrograph as a means to minimize fluorescence but nonetheless it is clear that any phosphorescence must be extremely weak. There is, in fact, no obvious indication of room-temperature phosphorescence from the crystal in the spectral window from 1100 to 1600 nm (Figure 9).

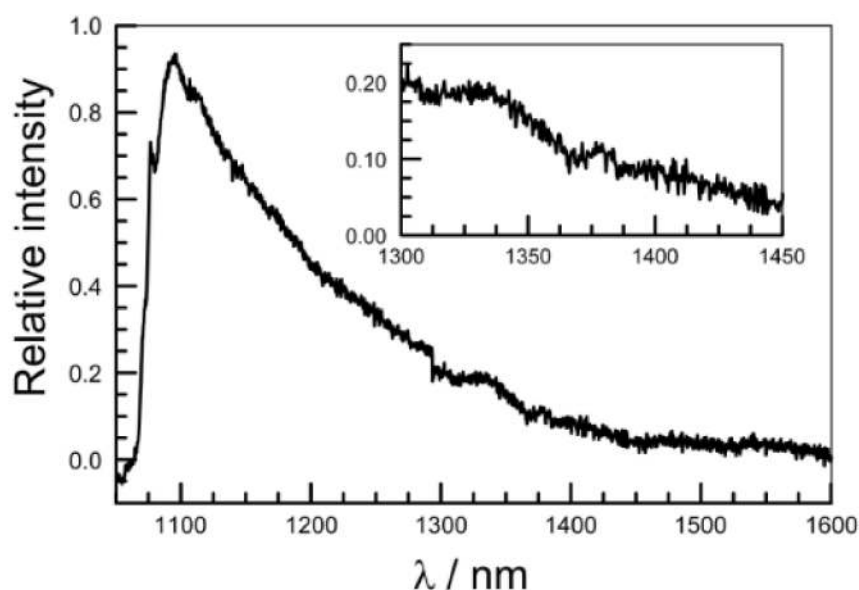


Figure 9. Emission spectrum recorded from a crystal of TIPS-P immersed in water and illuminated with a continuous wave laser at 532 nm (2 mW). The inset shows an expansion of the spectrum across the wavelength range of interest. A blocking filter was used to exclude emission at wavelengths <985 nm reaching the NIR detector and this is responsible for what might appear to be a peak at ca. 1100 nm. In the absence of the filter, emission intensity continues to increase with decreasing wavelength. The data acquisition time was 1 s.

3.3. Fluorescence from Concentrated Solution

Given the nature of the SEF process, it is natural to consider that the mechanism includes a role for intermolecular interactions between pairs of molecules as is well known for excimer and exciplex intermediates. Indeed, Guldi et al. [57] have made an eloquent case for the intermediacy of an intermolecular excimer during SEF for covalently-linked non-symmetrically substituted, pentacene-based bichromophores. An excimer intermediate has also been implicated in SEF occurring in thin films prepared from 1,3-diphenylisobenzofuran, as reported by Michl et al. [58]. Interestingly, slight variations in the molecular topology of relatively amorphous films, due to a change in substitution pattern, allows excimer formation to compete effectively with SEF for certain alkyl-substituted 1,3-diphenylisobenzofurans [59]. A similar situation holds for brominated perylene diimides where structural disruption of the amorphous film results in efficient SEF due to inhibition of competing excimer formation [60]. A clear-cut case for excimer formation competing with SEF has been made for TIPS-tetracene in concentrated solution [61]. In this case, SEF is an endergonic process, unlike with TIPS-P. The likely roles for charge transfer and excimer formation have also been elucidated for SEF in rylene and diketopyrrolopyrrole derivatives [62]. Of direct relevance to the present work is the report [18] that TIPS-P undergoes SEF in highly concentrated toluene solution, where the TIPS groups help to solubilize the solute and hinder close association between adjacent molecules [14]. In this case, it is reported [18] that triplet multiplication proceeds by way of a fluorescent excimer [18]. There are, of course, well known problems, such as self-absorption, that complicate optical studies for highly concentrated solutions. To minimize such artefacts (Figure 10), we constructed a variable path length optical cell that allows a fixed absorbance over an inordinately wide concentration range. In fact, the path length could be varied systematically from 5 cm to less than 20 μm (Figure 11). Using this cell, we were able to show that the absorption spectrum for TIPS-P in toluene is independent of concentration over the range from 10^{-8} M to 0.11 M. The spectra show no sign of aggregation and no obvious broadening of the absorption bands at high concentration (Figure 10). This finding is in agreement with an earlier report [18].

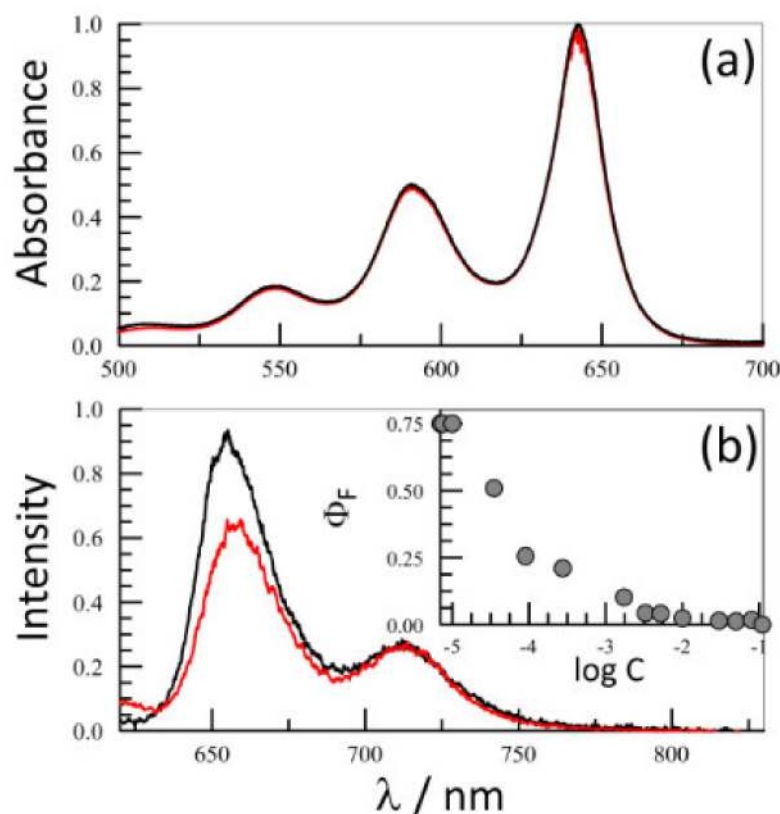


Figure 10. (a) Comparison of absorption spectra recorded for TIPS-P in toluene at concentrations of 1 μM (black curve) and 0.05 M (red curve). The spectra, which have been normalized at the respective maxima, were recorded with a variable path length optical cell to maintain a constant absorbance at any given wavelength. (b). Examples of fluorescence spectra recorded for the above solutions, with excitation at 595 nm and the same colour scheme. Note the minor distortion of the spectrum at high concentration caused by uncompensated self-absorption. The inset shows the effect of TIPS-P concentration on the fluorescence quantum yield.

Using the same cell, the fluorescence spectrum recorded at low (i.e., 10^{-7} M) concentration was identical to that described earlier in this manuscript. The fluorescence lifetime measured in air-equilibrated toluene was 13.3 ns. The fluorescence spectrum remains similar but not identical over the concentration range covering 10^{-7} M to 0.05 M. At the highest concentration, the higher-energy region (i.e., the 0,0 transition) shows minor distortion due to the onset of self-absorption. This effect becomes apparent from the slight red shift for the emission maximum (Figure 10). The short path length kept the degree of distortion to a minimum but there is no obvious contribution to the steady-state spectrum from excimer emission (Figure 10).

At low concentrations ($[\text{TIPS-P}] < 5 \mu\text{M}$), Φ_{F} remains constant at 0.75 in air-equilibrated toluene. This value begins to fall precipitously as the solute concentration exceeds ca. 20 μM . At the highest concentration that could be reached ($[\text{TIPS-P}] = 0.11$ M), fluorescence could barely be detected above the baseline. Time-resolved fluorescence decay curves could not be properly analyzed as single-exponential fits over the concentration range from 1 mM to 50 mM. Modelling the decay curves as the sum of two-exponential components gave greatly improved fits, as did the use of the stretched exponential function. In general, at high concentration, the decay curves correspond to a short-lived species with a lifetime of 240 ± 60 ps. This species dominates the total signal but there is always a minor contribution from a species having a lifetime in excess of 1 ns. For example, the best statistical fit obtained at a TIPS-P concentration of 12 mM corresponds to lifetimes of 225 ps (88%) and 1.65 ns (12%).



Figure 11. Photograph of the variable path length optical cell used to record the effect of solute concentration on the absorption and fluorescence spectral properties of TIPS-P in toluene. A screw barrel allows easy variation of the path length while the double seal prevents leakage of solution. The set-up fits comfortably into a range of spectrophotometers. Calibration of the path length is made by reference to standard solutions and/or birefringence effects.

4. Discussion

We present herein an updated description of the photophysical properties for TIPS-P in dilute solution at ambient temperature. The information provided should enable refinement of analytical treatments of experimental data relating to SEF in certain bichromophores. In particular, molar absorption coefficients for excited-singlet and excited-triplet states are believed to be the most accurate yet reported for TIPS-P. Our measured excited-state lifetimes are slightly longer than literature values and, at least in the case of the isolated triplet, reflect the low concentration of chromophore used for the measurement. We have also refined the molar absorption coefficient for the ground-state species, which is of critical importance in making quantitative SEF measurements since it is often used as the primary reference point. An important conclusion to emerge from this study concerns the inherent quantum yield for formation of the isolated triplet-excited state. Our results indicate that this value is less than a few percent (Table 2) in the absence of a spin-orbit accelerant. The dominant photoprocess is fluorescence, for which the quantum yield is 75% in air-equilibrated toluene – rising to 92% in the absence of molecular oxygen. This quenching by O_2 is attributed to the paramagnetic effect and leads to slight enhancement of the triplet yield.

The parameter of most significance is the excitation energy (E_T) of the isolated triplet state. We have not observed clear evidence for phosphorescence from TIPS-P in the region around 1400–1600 nm. Earlier work has reported phosphorescence at 1300 nm for pentacene (Pn) in frozen cyclohexane [27] and at 1580 nm for TIPS-P in frozen toluene [29] and in a 2-methyltetrahydrofuran glass at 77K [19]. These measurements, which are supported by various quantum chemical calculations [3,11,32] and indirect experimental observations [63,64], can be used to establish E_T values of 7700 cm^{-1} (i.e., 0.95 eV) for Pn and 6330 cm^{-1} (i.e., 0.78 eV) for TIPS-P. It might be noted that, rather than attempt to refine E_T , more recent theoretical studies have focused on diffusion of triplet states in solid materials [11] and distinguishing between isolated triplet and triplet biexcitons [12]. Our understanding of the protocol used for recording low-temperature phosphorescence from Pn [27] is that a conventional

fluorescence spectrophotometer, equipped with an immersion-well Dewar flask, was utilized. There is no indication that the optics or detector were modified to allow measurements in the NIR. Although no actual spectrum was provided, the reported emission maximum of 1300 nm matches with the expected appearance of the first overtone for the fluorescence peak, which can be a problem if inappropriate optical components are used. Given the tendency for Pn to aggregate, the low inherent Φ_T , and the (apparent) insensitivity of the instrument, we are reluctant to attach much significance to this particular measurement.

A second study [29] reports phosphorescence from TIPS-P in deoxygenated toluene at 77K. Here, the solubility is not an issue but toluene forms an ice at 77K that lacks good spectroscopic properties. We have shown, in confirmation of earlier work [20], that the inherent Φ_T for TIPS-P is low and we would not expect much triplet formation under these conditions. The radiative rate constants for the T_1 state of polyacenes are not expected to exceed a value of ca. 100 s^{-1} such that, for a phosphorescence lifetime of ca. $10 \text{ }\mu\text{s}$, the overall quantum yield for triplet emission will be less than ca. 10^{-5} , making detection difficult. This study [29] provided the phosphorescence spectrum for TIPS-P, together with spectra for a series of heteroacenes mostly related to TIPS-P. The spectra are similar and closely comparable to a second literature example [19]. Both studies conclude that E_T for TIPS-P is ca. 6330 cm^{-1} (i.e., 0.78 eV). This is well below the value for Pn and significantly less than one-half of the singlet excitation energy of 1.92 eV. More importantly for the present discussion, the reported phosphorescence energy is much smaller than our derived E_T of 7940 cm^{-1} (i.e., 0.98 eV) as derived by photoacoustic calorimetry. The discrepancy is well outside the limits of experimental error. Moreover, our mean E_T value marginally exceeds one-half of the singlet excitation energy and is therefore inconsistent with strongly exergonic SEF. It might be stressed at this point that highly efficacious SEF will produce a triplet biexciton and not the isolated triplet examined here.

At this point, it is worthwhile to re-iterate how the E_T value was reached. The triplet-excited state of TIPS-P was populated by way of triplet-triplet energy transfer using redaporfin ($E_T = 9090 \text{ cm}^{-1}$) as energy donor. The experiment measures heat released within a fairly narrow time window of 20 ns to $1 \text{ }\mu\text{s}$. The set-up does not monitor deactivation of the T_1 state of TIPS-P formed via energy transfer but does detect the enthalpy change associated with the electronic energy transfer step. Thus, the primary measurement refers to the difference in triplet excitation energies between donor and acceptor. The amount of heat released during this step is smaller than expected if SEF is exergonic, although taking the lower limit set by experimental uncertainty (i.e., $E_T = 6750 \text{ cm}^{-1}$) overcomes this obstacle. We have no reason to doubt the photophysical properties attributed to redaporfin and therefore are at a loss to satisfactorily resolve this apparent discrepancy in E_T values. Possible complications for the energy-transfer step that could decrease the apparent energy gap between the triplet states, such as transfer to T_2 rather than T_1 or preferential population of a "hot" vibronic state for the acceptor triplet, do not appear feasible. The T_2 state is thought to be closer in energy to S_1 than to T_1 [28] and therefore would not be accessible to the triplet state of redaporfin. The T_1 state of TIPS-P does not generate the characteristic luminescence signal for singlet molecular oxygen when illuminated at 532 nm in O_2 -saturated toluene, indicating that E_T is below the excitation energy of 7875 cm^{-1} for molecular oxygen. We will describe in a separate publication phosphorescence recorded following excitation of a TIPS-P-based bichromophore, the same molecule as studied earlier by pulse radiolysis [22], at room temperature. The emission peak, observed with two different instruments operated under quite disparate conditions, attributed to the isolated triplet occurs at 1370 nm (i.e., 7290 cm^{-1}). This additional E_T value is within experimental error of that measured by photoacoustic calorimetry and meets all of the required criteria.

A second important feature to emerge from our study concerns excimer fluorescence from TIPS-P at high concentration in liquid solution. Two literature reports describe excimer emission in toluene solution [18,29] but the exhibited spectra bear all the classical hallmarks of self-absorption. This is a very well-established problem for highly concentrated media, being a particular problem for chlorophyll [65], and leads to a progressive red shift with increasing chromophore concentration. The origin of this

spectral shift is the effective disappearance of the 0,0 fluorescence band due to absorption by the ground-state chromophore. Self-absorption is a particular problem for compounds exhibiting a small Stokes shift and a strong 0,0 absorption band! It has already been recognized as being responsible for distorting the fluorescence spectrum of TIPS-P in concentrated solutions [30]. Our variable path length optical cell helps overcome this problem by maintaining the same absorbance at all concentrations. Even at 0.11 M, we were unable to confirm excimer fluorescence for TIPS-P in toluene. This is not to say that an excimer is not involved in SEF, especially in endergonic cases such as with TIPS-tetracene [60], but we are of the opinion that there is no excimer emission for highly concentrated solutions of TIPS-P. The strong fluorescence quenching observed at high concentration could contain an important contribution from SEF [18].

The final point of interest relates to fluorescence from single crystals of TIPS-P. It is recognized that solid-state samples of Pn are often very weakly fluorescent [3], although intense and sharp fluorescence has been reported for Pn monolayers grown on polymeric surfaces [66]. We have found difficulties for recording high quality fluorescence spectra for sublimed films and drop-cast films of Pn after drying under high vacuum. Our crystals of TIPS-P are weakly fluorescent, displaying an emission spectrum that resembles that found in dilute solution and in monolayers [66]. This observation is explained in terms of the sample comprising two main domains; one such region has crystalline character while the other is more amorphous. Fluorescence and laser ablation occur primarily from amorphous regions while SEF is more likely associated with the crystalline domain. Prior work has already commented on sub-domain spectroscopy for TIPS-P [56]. Our failure to detect room-temperature phosphorescence in the NIR region, despite facile detection of the tail of the fluorescence spectrum, indicates that, under such conditions, the phosphorescence quantum yield must be less than 10^{-6} .

Author Contributions: A.A. synthesized, characterized and purified samples of target compounds: J.K.G.K. designed and performed the photophysical studies and, in conjunction with A.H., carried out the data analysis: L.G.A. designed and constructed the PAC apparatus and conceived the PAC experiments. F.A.S. and C.S. carried out the PAC studies and, together with L.G.A., completed the data analysis: J.K.G.K. designed the variable path length cell and conceived the concentration dependence studies: A.D.W. designed and configured the microscope, optics and spectrometer for NIR emission studies and, together with A.H., acquired and analyzed the NIR emission data. A.H. wrote the initial draft of the ms, with input from L.G.A. and A.D.W. All authors have read and agreed to the final version of the manuscript.

Funding: We thank Newcastle University and Coimbra University for providing access to key facilities to undertake this research project. We also thank STFC CLF Octopus Facility for PoC access to the NIR emission microscope. Thanks are due to Luzitin S.A. for providing a sample of redaporfin. We acknowledge financial support from the Portuguese Science Foundation (UIDB/QUI/00313/2020, Roteiro/0152/2013/022124) and from the European Union's Horizon 2020 Research and Innovation Programme under grant agreement no. 654148 Laser Lab-Europe. AA thanks TUBITAK (The Scientific and Technological Research Council of Turkey) for the award of a research fellowship.

Acknowledgments: We thank John Corner and Gary Day for advice about the design and for construction of the variable path length optical cell.

Conflicts of Interest: The authors declare no conflict of interest.

References

1. Greyson, E.C.; Stepp, B.R.; Chen, X.D.; Schwerin, A.F.; Paci, I.; Smith, M.B.; Akdag, A.; Johnson, J.C.; Nozik, A.J.; Michl, J.; et al. Singlet exciton fission for solar cell applications. Energy aspects of interchromophore coupling. *J. Phys. Chem.* **2010**, *114*, 14223–14232. [[CrossRef](#)] [[PubMed](#)]
2. Smith, M.B.; Michl, J. Recent advances in singlet fission. *Ann. Rev. Phys. Chem.* **2013**, *64*, 361–386. [[CrossRef](#)] [[PubMed](#)]
3. Smith, M.B.; Michl, J. Singlet fission. *Chem. Rev.* **2010**, *110*, 6891–6936. [[CrossRef](#)] [[PubMed](#)]
4. Thampi, A.; Stern, H.L.; Cheminal, A.; Tayebjee, M.J.Y.; Petty, A.J., II; Anthony, J.E.; Rao, A. Elucidation of excitation energy dependent correlated triplet pair formation pathways in an endothermic singlet fission system. *J. Am. Chem. Soc.* **2018**, *140*, 4613–4622. [[CrossRef](#)]
5. Berkelbach, T.C.; Hybertsen, M.S.; Reichman, D.R. Microscopic theory of singlet exciton fission. II. Application to pentacene dimers and the role of superexchange. *J. Chem. Phys.* **2013**, *138*, 114103. [[CrossRef](#)]

6. Busby, E.; Berkelbach, T.C.; Kumar, B.; Chernikov, A.; Zhong, Y.; Zhu, X.-Y.; Heinz, T.F.; Hybertsen, M.S.; Sfeir, M.Y.; Reichman, D.R.; et al. Multiphonon relaxation slows singlet fission in crystalline hexacene. *J. Am. Chem. Soc.* **2014**, *136*, 10654–10660. [[CrossRef](#)]
7. Ryerson, J.L.; Zaykov, A.; Suarez, L.E.A.; Havenith, R.W.A.; Stepp, B.R.; Dron, P.I.; Kaleta, J.; Akdag, A.; Teat, S.J.; Magnera, T.F.; et al. Structure and photophysics of indigoids for singlet fission: Cibalackrot. *J. Chem. Phys.* **2019**, *151*, 184903. [[CrossRef](#)]
8. Buchanan, E.A.; Michl, J. Optimal arrangements of 1,3-diphenylisobenzofuran molecule pairs for fast singlet fission. *Photochem. Photobiol. Sci.* **2019**, *18*, 2112–2124. [[CrossRef](#)]
9. Johnson, J.C.; Nozik, A.J.; Michl, J. The role of chromophore coupling in singlet fission. *Acc. Chem. Res.* **2013**, *46*, 1290–1299. [[CrossRef](#)]
10. Wu, Y.; Liu, K.; Liu, H.; Zhang, Y.; Zhang, H.; Yao, J.; Fu, H. Impact of intermolecular distance on singlet fission in a series of TIPS pentacene compounds. *J. Phys. Chem. Lett.* **2014**, *5*, 3451–3455. [[CrossRef](#)]
11. Miyata, K.; Conrad-Burton, F.S.; Geyer, F.L.; Zhu, X.-Y. Triplet pair states in singlet fission. *Chem. Rev.* **2019**, *119*, 4261–4292. [[CrossRef](#)] [[PubMed](#)]
12. Khan, S.; Mazumdar, S. Theory of transient excited state absorptions in pentacene and derivatives: Triplet–triplet biexciton versus free triplets. *J. Phys. Chem. Lett.* **2017**, *8*, 5943–5948. [[CrossRef](#)] [[PubMed](#)]
13. Greyson, E.C.; Vura-Weis, J.; Michl, J.; Ratner, M.A. Maximizing singlet fission in organic dimers. Theoretical investigation of triplet yield in the regime of localized excitation and fast coherent electron transfer. *J. Phys. Chem.* **2010**, *114*, 14168–14177. [[CrossRef](#)] [[PubMed](#)]
14. Anthony, J.E.; Brooks, J.S.; Eaton, D.L.; Parkin, S.R. Functionalized pentacene: Improved electronic properties from control of solid-state order. *J. Am. Chem. Soc.* **2001**, *123*, 9482–9483. [[CrossRef](#)]
15. Sheraw, C.D.; Jackson, T.N.; Eaton, D.L.; Anthony, J.E. Functionalized pentacene active layer organic thin-film transistors. *Adv. Mater.* **2003**, *15*, 2009–2011. [[CrossRef](#)]
16. Yang, L.; Tabachnyk, M.; Bayliss, S.L.; Bohm, M.L.; Broch, K.; Greenham, N.C.; Friend, R.H.; Ehrler, B. Solution-Processable Singlet Fission Photovoltaic Devices. *Nano Lett.* **2015**, *15*, 354–358. [[CrossRef](#)]
17. Ramanan, C.; Smeigh, A.L.; Anthony, J.E.; Marks, T.J.; Wasielewski, M.R. Competition between singlet fission and charge separation in solution-processed blend films of 6,13-bis(triisopropylsilylethynyl)pentacene with sterically-encumbered perylene-3,4:9,10-bis(dicarboximide)s. *J. Am. Chem. Soc.* **2012**, *134*, 386–397. [[CrossRef](#)]
18. Walker, B.J.; Musser, A.J.; Beljonne, D.; Friend, R.H. Singlet exciton fission in solution. *Nat. Chem.* **2013**, *5*, 1019–1024. [[CrossRef](#)]
19. Zirzmeier, J.; Lehnher, D.; Coto, P.B.; Chernick, E.T.; Casillas, R.; Basel, B.S.; Thoss, M.; Tykwinski, R.R.; Guldi, D.M. Singlet fission in pentacene dimers. *Proc. Natl. Acad. Sci. USA* **2015**, *112*, 5325–5330. [[CrossRef](#)]
20. Alagna, N.; Lustres, J.L.P.; Wollscheid, N.; Luo, Q.Q.; Han, J.; Dreuw, A.; Geyer, F.L.; Brosius, V.; Bunz, U.H.F.; Backup, T.; et al. Singlet fission in tetraaza-TIPS-pentacene oligomers: From fs excitation to μ s triplet decay via the biexcitonic state. *J. Phys. Chem.* **2019**, *123*, 10780–10793. [[CrossRef](#)]
21. Sakuma, T.; Sakai, H.; Araki, Y.; Mori, T.; Wada, T.; Tkachenko, N.V.; Hasobe, T. Long-lived triplet excited states of bent-shaped pentacene dimers by intramolecular singlet fission. *J. Phys. Chem.* **2016**, *120*, 1867–1875. [[CrossRef](#)] [[PubMed](#)]
22. Karlsson, J.K.G.; Atahan, A.; Harriman, A.; Tojo, S.; Fujitsuka, M.; Majima, T. Pulse radiolysis of TIPS-pentacene and a fluorene-bridged bis(pentacene): Evidence for intramolecular singlet-exciton fission. *J. Phys. Chem. Lett.* **2018**, *9*, 3934–3938. [[CrossRef](#)] [[PubMed](#)]
23. Herz, J.; Backup, T.; Paulus, F.; Engelhart, J.U.; Bunz, U.H.F.; Motzkus, M. Unveiling singlet fission mediating states in TIPS-pentacene and its aza derivatives. *J. Phys. Chem. A* **2015**, *119*, 6602–6610. [[CrossRef](#)] [[PubMed](#)]
24. Korovina, N.; Pompetti, N.; Johnson, J.C. Lessons from intramolecular singlet fission with covalently bound chromophores. *J. Chem. Phys.* **2020**, *152*, 040904. [[CrossRef](#)] [[PubMed](#)]
25. Stern, H.L.; Musser, A.J.; Gelinas, S.; Parkinson, P.; Herz, L.M.; Bruzek, M.J.; Anthony, J.; Friend, R.H.; Walker, B.J. Identification of a triplet pair intermediate in singlet exciton fission in solution. *Proc. Natl. Acad. Sci. USA* **2015**, *112*, 7656–7661. [[CrossRef](#)] [[PubMed](#)]
26. Eaton, S.W.; Shoer, L.E.; Karlen, S.D.; Dyar, S.M.; Margulies, E.A.; Veldkamp, B.S.; Ramanan, C.; Hartzler, D.A.; Savikhin, S.; Marks, T.J.; et al. Singlet exciton fission in polycrystalline thin films of a slip-stacked perylenediimide. *J. Am. Chem. Soc.* **2013**, *135*, 14701–14712. [[CrossRef](#)]

27. Nijegorodov, N.; Ramachandran, V.; Winkoun, D.P. The dependence of the absorption and fluorescence parameters, the intersystem crossing and internal conversion rate constants on the number of rings in polyacene molecules. *Spectrochim. Acta Part A: Mol. Biomol. Spectr.* **1997**, *53*, 1813–1824. [[CrossRef](#)]
28. Zimmerman, P.M.; Zhang, Z.; Musgrave, C.B. Singlet fission in pentacene through multi-exciton quantum states. *Nat. Chem.* **2010**, *2*, 648–652. [[CrossRef](#)]
29. Zhang, Y.-D.; Wu, Y.; Xu, Y.; Wang, Q.; Liu, K.; Chen, J.-W.; Cao, J.J.; Zhang, C.; Fu, H.; Zhang, H.-L. Excessive exoergicity reduces singlet exciton fission efficiency of heteroacenes in solutions. *J. Am. Chem. Soc.* **2016**, *138*, 6739–6745. [[CrossRef](#)]
30. Grieco, C.; Doucette, G.S.; Munson, K.T.; Swartzfager, J.R.; Munro, J.M.; Anthony, J.E.; Dabo, I.; Asbury, J.B. Vibrational probe of the origin of singlet exciton fission in TIPS-pentacene solutions. *J. Chem. Phys.* **2019**, *151*, 154701. [[CrossRef](#)]
31. Yago, T.; Ishikawa, K.; Katoh, R.; Wakasa, M. Magnetic field effects on triplet pair generated by singlet fission in an organic crystal: Application of radical pair model to triplet pair. *J. Phys. Chem. C* **2016**, *120*, 27858–27870. [[CrossRef](#)]
32. Kaur, I.; Jia, W.; Kopreski, R.P.; Selvarasah, S.; Dokmeci, M.R.; Pramanik, C.; McGruer, N.E.; Miller, G.P. Substituent effects in pentacenes: Gaining control over HOMO-LUMO gaps and photooxidative processes. *J. Am. Chem. Soc.* **2008**, *130*, 16274–16286. [[CrossRef](#)] [[PubMed](#)]
33. Seybold, P.G.; Gouterman, M. Porphyrins XIII: Fluorescence spectra and quantum yields. *J. Mol. Spectrosc.* **1969**, *31*, 1–13. [[CrossRef](#)]
34. Pineiro, M.; Gonsalves, A.M.D.R.; Pereira, M.M.; Formosinho, S.J.; Arnaut, L.G. New halogenated phenylbacteriochlorins and their efficiency in singlet-oxygen sensitization. *J. Phys. Chem.* **2002**, *106*, 3787–3795. [[CrossRef](#)]
35. De Melo, J.S.S.; Burrows, H.D.; Serpa, C.; Arnaut, L.G. The triplet state of indigo. *Angew. Chem. Int. Ed.* **2007**, *46*, 2094–2096. [[CrossRef](#)] [[PubMed](#)]
36. Gomes, P.J.S.; Serpa, C.; Arnaut, L.G. About biphenyl first excited triplet state energy. *J. Photochem. Photobiol. Chem.* **2006**, *184*, 228–233. [[CrossRef](#)]
37. Gallimore, P.J.; Davidson, N.M.; Kalberer, M.; Pope, F.D.; Ward, A.D. 1064 nm Dispersive Raman microspectroscopy and optical trapping of pharmaceutical aerosols. *Anal. Chem.* **2018**, *90*, 8838–8844. [[CrossRef](#)]
38. Strickler, S.J.; Berg, R.A. Relationship between absorption intensity and fluorescence lifetime of molecules. *J. Chem. Phys.* **1962**, *37*, 814–822. [[CrossRef](#)]
39. Zeng, Y.; Biczok, L.; Linschitz, H. External heavy-atom induced phosphorescence emission of fullerenes—The energy of triplet C-60. *J. Phys. Chem.* **1992**, *96*, 5237–5239. [[CrossRef](#)]
40. Porter, G.; Wilkinson, F. Energy transfer from the triplet state. *Proc. R. Soc. Lond.* **1961**, *264*, 1–18. [[CrossRef](#)]
41. Arnaut, L.G.; Pereira, M.M.; Dabrowski, J.M.; Silva, E.F.F.; Schaberle, F.A.; Abreu, A.R.; Rocha, L.B.; Barsan, M.M.; Urbanska, K.; Stochel, G.; et al. Photodynamic therapy efficacy enhanced by dynamics: The role of charge transfer and photostability in the selection of photosensitizers. *Chem. Eur. J.* **2014**, *20*, 5346–5357. [[CrossRef](#)] [[PubMed](#)]
42. Schaberle, F.A.; Abreu, A.R.; Gonçalves, P.F.; Sá, G.F.F.; Pereira, M.M.; Arnaut, L.G. Ultrafast dynamics of manganese(III), manganese(II), and free-base bacteriochlorin: Is there time for photochemistry? *Inorg. Chem.* **2017**, *56*, 2677–2689. [[CrossRef](#)] [[PubMed](#)]
43. Arnaut, L.G.; Caldwell, R.A.; Elbert, J.E.; Melton, L.A. Recent advances in photoacoustic calorimetry—Theoretical basis and improvements in experimental design. *Rev. Sci. Instrum.* **1992**, *63*, 5381–5389. [[CrossRef](#)]
44. Schaberle, F.A.N.; Nunes, R.M.D.; Barroso, M.; Serpa, C.; Arnaut, L.G. Analytical solution for time-resolved photoacoustic calorimetry data and applications to two typical photoreactions. *Photochem. Photobiol. Sci.* **2010**, *9*, 812–822. [[CrossRef](#)]
45. Braslavsky, S.E.; Heibel, G.E. Time-resolved photothermal and photoacoustic methods applied to photoinduced processes in solution. *Chem. Rev.* **1992**, *92*, 1381–1410. [[CrossRef](#)]
46. Pineiro, M.; Carvalho, A.L.; Pereira, M.M.; Gonsalves, A.M.D.R.; Arnaut, L.G.; Formosinho, S. Photoacoustic measurements of porphyrin triplet-state quantum yields and singlet-oxygen efficiencies. *Chem. Eur. J.* **1998**, *4*, 2299–2307. [[CrossRef](#)]

47. Schaberle, F.A.; Rego Filho, F.A.M.G.; Reis, L.A.; Arnaut, L.G. Assessment of lifetime resolution limits in time-resolved photoacoustic calorimetry vs. transducer frequencies: Setting the stage for picosecond resolution. *Photochem. Photobiol. Sci.* **2016**, *15*, 204–210. [[CrossRef](#)]
48. Levy, D.; Avnir, D. Room-temperature phosphorescence and delayed fluorescence of organic molecules trapped in silica sol-gel glasses. *J. Photochem. Photobiol. Chem.* **1991**, *57*, 41–63. [[CrossRef](#)]
49. Lubert-Perquel, D.; Salvadori, E.; Dyson, M.; Stavrinou, P.N.; Montis, R.; Nagashima, H.; Kobori, Y.; Heutz, S.; Kay, C.W.M. Identifying triplet pathways in dilute pentacene films. *Nat. Commun.* **2018**, *9*, 4222. [[CrossRef](#)]
50. Niu, M.S.; Zheng, F.; Yang, X.Y.; Bi, P.Q.; Feng, L.; Hao, X.T. Molecular packing correlated fluorescence in TIPS-pentacene films. *Org. Electron.* **2017**, *49*, 340–346. [[CrossRef](#)]
51. Grieco, C.; Doucette, G.S.; Pensack, R.D.; Payne, M.M.; Rimshaw, A.; Scholes, G.D.; Anthony, J.E.; Asbury, J.B. Dynamic exchange during triplet transport in nanocrystalline TIPS-pentacene films. *J. Am. Chem. Soc.* **2016**, *138*, 16069–16080. [[CrossRef](#)] [[PubMed](#)]
52. Sharifzadeh, S.; Wong, C.Y.; Wu, H.; Cotts, B.L.; Kronik, L.; Ginsberg, N.S.; Neaton, J.B. Relating the physical structure and optoelectronic function of crystalline TIPS-pentacene. *Adv. Funct. Mater.* **2015**, *25*, 2038–2046. [[CrossRef](#)]
53. Wilson, M.W.B.; Rao, A.; Ehrler, B.; Friend, R.H. Singlet exciton fission in polycrystalline pentacene: From photophysics toward devices. *Acc. Chem. Res.* **2013**, *46*, 1330–1338. [[CrossRef](#)] [[PubMed](#)]
54. Tayebjee, M.J.Y.; Schwarz, K.N.; MacQueen, R.W.; Dvorak, M.; Lam, A.W.C.; Ghiggino, K.P.; McCamey, D.R.; Schmidt, T.W.; Conibeer, G.J. Morphological evolution and singlet fission in aqueous suspensions of TIPS-pentacene nanoparticles. *J. Phys. Chem.* **2016**, *120*, 157–165. [[CrossRef](#)]
55. Platt, A.D.; Day, J.; Subramanian, S.; Anthony, J.E.; Ostroverkhova, O. Optical, fluorescent, and (photo)conductive properties of high-performance functionalized pentacene and anthradithiophene derivatives. *J. Phys. Chem.* **2009**, *113*, 14006–14014. [[CrossRef](#)]
56. Wong, C.Y.; Penwell, S.B.; Cotts, B.L.; Noriega, R.; Wu, H.; Ginsberg, N.S. Revealing exciton dynamics in a small-molecule organic semiconducting film with subdomain transient absorption microscopy. *J. Phys. Chem.* **2013**, *117*, 22111–22122. [[CrossRef](#)]
57. Casillas, R.; Adam, M.; Coto, P.B.; Waterloo, A.R.; Zirzmeier, J.; Reddy, S.R.; Hampel, F.; McDonald, R.; Tykwinski, R.R.; Thoss, M.; et al. Intermolecular singlet fission in unsymmetrical derivatives of pentacene in solution. *Adv. Ener. Mater.* **2019**, *9*, 1802221. [[CrossRef](#)]
58. Schrauben, J.N.; Ryerson, J.L.; Michl, J.; Johnson, J.C. Mechanism of singlet fission in thin films of 1,3-diphenylisobenzofuran. *J. Amer. Chem. Soc.* **2014**, *136*, 7363–7373. [[CrossRef](#)]
59. Dron, P.I.; Michl, J.; Johnson, J.C. Singlet fission and excimer formation in disordered solids of alkyl-substituted 1,3-diphenylisobenzofurans. *J. Phys. Chem. A* **2017**, *121*, 8596–8603. [[CrossRef](#)]
60. Felter, K.M.; Dubey, R.K.; Grozema, F.C. Relation between molecular packing and singlet fission in thin films of brominated perylenediimides. *J. Chem. Phys.* **2019**, *151*, 094301. [[CrossRef](#)]
61. Dover, C.B.; Gallaher, J.K.; Frazer, L.; Tapping, P.C.; Petty, A.J.; Crossley, M.J.; Anthony, J.E.; Kee, T.W.; Schmidt, T.W. Endothermic singlet fission is hindered by excimer formation. *Nat. Chem.* **2018**, *10*, 305–310. [[CrossRef](#)]
62. Miller, C.E.; Wasielewski, M.R.; Schatz, G.C. Modeling singlet fission in rylene and diketopyrrolopyrrole derivatives: The role of the charge transfer state in superexchange and excimer formation. *J. Phys. Chem. C* **2017**, *121*, 10345–10350. [[CrossRef](#)]
63. Burgos, J.; Pope, M.; Swenberg, C.E.; Alfano, R.R. Hetero-fission in pentacene-doped tetracene single crystals. *Phys. Status Solidi* **1977**, *83*, 249–256. [[CrossRef](#)]
64. Friend, R.H.; Phillips, M.; Rao, A.; Wilson, M.W.N. Excitons and charges at organic semiconductor heterojunctions. *Faraday Discuss.* **2012**, *155*, 339–348. [[CrossRef](#)] [[PubMed](#)]
65. Weis, E. Chlorophyll fluorescence at 77K in intact leaves—Characterization of a technique to eliminate artifacts related to self-absorption. *Photosynthesis Res.* **1985**, *6*, 73–86. [[CrossRef](#)]
66. He, R.; Tassi, N.G.; Blanchet, G.B.; Pinczuk, A. Intense photoluminescence from pentacene monolayers. *Appl. Phys. Lett.* **2010**, *96*, 263303. [[CrossRef](#)]

